

# SCIENTIFIC REPORTS



OPEN

## A nano-silicate material with exceptional capacity for CO<sub>2</sub> capture and storage at room temperature

Leide P. Cavalcanti<sup>1</sup>, Georgios N. Kalantzopoulos<sup>2</sup>, Juergen Eckert<sup>3</sup>, Kenneth D. Knudsen<sup>1,4</sup> & Jon Otto Fossum<sup>4</sup>

In order to mitigate climate change driven by the observed high levels of carbon dioxide (CO<sub>2</sub>) in the atmosphere, many micro and nano-porous materials are being investigated for CO<sub>2</sub> selectivity, capture and storage (CCS) purposes, including zeolites, metal organic frameworks (MOFs), functionalized polymers, activated carbons and nano-silicate clay minerals. Key properties include availability, non-toxicity, low cost, stability, energy of adsorption/desorption, sorbent regeneration, sorption kinetics and CO<sub>2</sub> storage capacity. Here, we address the crucial point of the volumetric capture and storage capacity for CO<sub>2</sub> in a low cost material which is natural, non-toxic, and stable. We show that the nano-silicate Nickel Fluorohectorite is able to capture 0.79 metric tons of CO<sub>2</sub> per m<sup>3</sup> of host material - one of the highest capacities ever achieved - and we compare volumetric and gravimetric capacity of the best CO<sub>2</sub> sorbent materials reported to date. Our results suggest that the high capture capacity of this fluorohectorite clay is strongly coupled to the type and valence of the interlayer cation (here Ni<sup>2+</sup>) and the high charge density, which is almost twice that of montmorillonite, resulting in the highest reported CO<sub>2</sub> uptake among clay minerals.

A current major challenge in science and technology is the development of low cost materials with large CO<sub>2</sub> capture and storage (CCS)<sup>1</sup> capacity, retention ability and sorption selectivity<sup>2</sup>. Important factors for the choice of material in this context include its availability, environmental friendliness, non-toxicity, a low level of greenhouse gas emission during processing, material stability, production cost, CO<sub>2</sub> storage capacity, energy of adsorption/desorption, sorbent regeneration, sorption kinetics and capacity per volume or per mass of host material. Many materials are being investigated including zeolites<sup>3</sup>, metal organic frameworks (MOFs)<sup>4</sup>, functionalized polymers<sup>5,6</sup>, activated carbons<sup>7</sup> and nano-silicate clay minerals<sup>8-10</sup>. Also hybrid solutions using the best characteristics among all these absorbents are much investigated<sup>11</sup>. This work presents a quantitative study of the capture of CO<sub>2</sub> by Fluorohectorite clay - a stable and low cost material - with different interlayer cations. Fluorohectorite clay is a modified hectorite clay, which is a species belonging to the smectite group<sup>12</sup>, classified as a 2:1 layered silicates, with layer periodicity of approximately 1 nm. The periodic structure includes an interlayer space where a cation is lodged, bonding the structure and balancing the overall charges. The group of smectites, commonly addressed in short as clays, also comprise more popular species like montmorillonite clays. The synthetic fluorohectorite, studied in the present work, has been demonstrated, in several publications by our group, to be a representative and clean model system of nano-silicate smectite clay minerals<sup>13</sup>. Synthetic nano-silicate clays contain significantly fewer impurities (e.g. carbonates, (hydr)oxides, silica, and organic matter) than natural clays and show a more homogenous charge distribution than their natural counterparts<sup>14</sup>, leading to well-defined intercalation states<sup>15,16</sup>. Intercalation of water in nano-silicate smectite clays occurs naturally and has been extensively studied with a wide range of techniques, among them neutron<sup>17,18</sup> and X-ray scattering<sup>13,19</sup>. Recent experiments and simulations have shown that also CO<sub>2</sub> can intercalate in smectite clays, both in supercritical<sup>20</sup>, and in gaseous/liquid form<sup>21</sup>. We have previously demonstrated<sup>22</sup> that under certain conditions of pressure and temperature, fluorohectorite clays

<sup>1</sup>Institute for Energy Technology (IFE), Kjeller, Norway. <sup>2</sup>Centre for Materials Science and Nanotechnology (SMN), Department of Chemistry, University of Oslo, Oslo, Norway. <sup>3</sup>University of South Florida (USF), Tampa, USA. <sup>4</sup>Norwegian University of Science and Technology (NTNU), Trondheim, Norway. Correspondence and requests for materials should be addressed to L.P.C. (email: [leide.cavalcanti@gmail.com](mailto:leide.cavalcanti@gmail.com)) or J.O.F. (email: [jon.fossum@ntnu.no](mailto:jon.fossum@ntnu.no))

Material	Gravimetric capacity		Molar Uptake	(d) Density (g/cm <sup>3</sup> )	Volumetric capacity	Final Pressure (bar)	Data
	Ratio (G) CO <sub>2</sub> (g)/Material(g)	Fraction CO <sub>2</sub> (g)/[CO <sub>2</sub> (g) + Material(g)]	(G*m) CO <sub>2</sub> (mmol)/Material(g)		(G*d) CO <sub>2</sub> (ton)/Material(m <sup>3</sup> )		
Clay NiFh (this work)	0.28	0.22	6.4	2.8	0.79 ± 0.02 <sup>†</sup>	55	exp
Clay NaFh (this work)	0.21	0.17	4.7	2.8	0.58 ± 0.02 <sup>†</sup>	53	exp
Clay LiFh (this work)	0.16	0.14	3.7	2.8	0.46 ± 0.02 <sup>†</sup>	53	exp
Montmorillonite CTAB N2 (Stevens, 2013)	<i>0.11</i>	<i>0.10</i>	<b>2.42</b>	2.8	<i>0.31</i>	<b>1</b>	<b>exp</b>
Zeolite 13X (Cavenati, 2004)	<i>0.32</i>	<i>0.24</i>	<b>7.372</b>	<b>1.130</b>	<i>0.35</i>	<b>32</b>	exp
co-IonomIM-17% (Mg <sup>2+</sup> ) (Rukmani, 2018)	<i>0.20</i>	<b>0.17</b>	<b>4.5</b>	<b>0.89</b>	<i>0.18</i>	<b>2</b>	<b>S</b>
MOF-aminoclay CuBTC@AC-2 (Chakraborty, 2016)	<i>0.24</i>	<i>0.19</i>	<b>5.4</b>	—	—	<b>1</b>	exp
mesoporous carbon MPPY4800 (Cox, 2017)	<b>2.42</b>	<i>0.71</i>	<b>54</b>	<i>0.38</i>	<b>0.93</b>	<b>50</b>	exp
MOF-210 (Furukawa, 2010; Sumida, 2012)	<b>2.87</b>	<b>0.74</b>	65	<b>0.25</b>	<i>0.72</i>	<b>50</b>	exp

**Table 1.** CO<sub>2</sub> intercalation values and clay parameters. **m** = 1000/Mw(CO<sub>2</sub>); <sup>†</sup>Error propagation considering ± 2% uncertainty in mass of clay sample and ± 10% in volume; **exp** = experimental result; **S** = simulation; The values in **bold** are from the cited references; the values in *italic* were determined for the sake of comparison in this table.

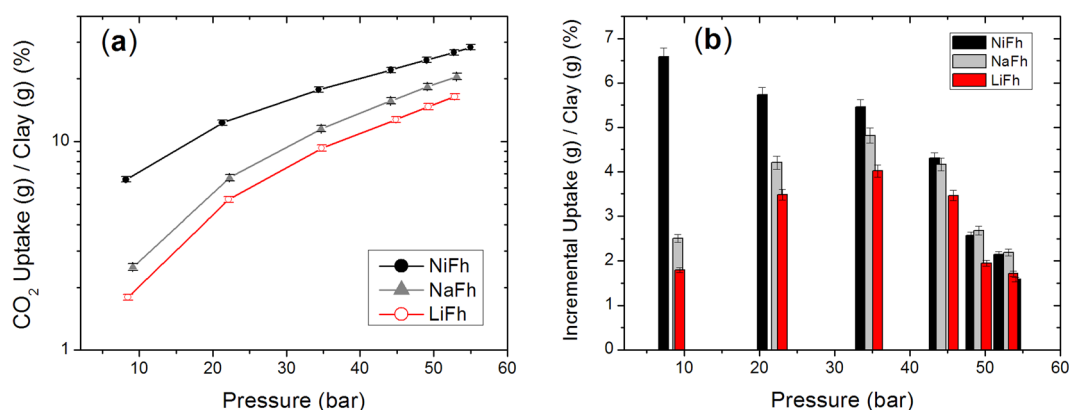


**Figure 1.** (a) Total uptake of CO<sub>2</sub> into Fluorohectorite nano-silicate clay minerals determined for each pressure step at room temperature; (b) Incremental uptake of CO<sub>2</sub> into Fluorohectorite clays for each pressure step.

can capture a large amount of CO<sub>2</sub> depending on the type of interlayer cation, and that Nickel-fluorohectorite clay (NiFh), in particular, will retain CO<sub>2</sub> up to a temperature of 35 °C at ambient pressure<sup>23</sup>. The captured CO<sub>2</sub> can subsequently be released by heating above this temperature. These conditions are highly relevant for mapping out and understanding the mechanisms involved in CO<sub>2</sub> capture and retention by nano-silicates, either in geological formations, or in technological CO<sub>2</sub> absorbent materials.

## Results and Discussion

We have utilized an accurately calibrated custom-made Sieverts apparatus for the quantification of CO<sub>2</sub> storage capacity of the nano-silicate clay minerals. The setup is described in detail in the Methods section. The high-pressure CO<sub>2</sub> uptake at room temperature (Fig. 1a) shows a maximum CO<sub>2</sub> intercalation of 28% in weight for NiFh clay at the final pressure of 55 bar. This value is equivalent to 6.45 mmol of CO<sub>2</sub> per gram of NiFh, which corresponds to 0.795 ton of CO<sub>2</sub> per m<sup>3</sup> of clay at 55 bar and room temperature, given the crystallographic density of the clay (2.8 g/ml). This result demonstrates that NiFh is able to intercalate one of the largest amounts of CO<sub>2</sub> per volume of material of all porous materials reported in literature. Commercially available zeolite<sup>3</sup> 13X can adsorb 0.35 ton/m<sup>3</sup>, the mesoporous carbon<sup>7</sup> MPPY-4800 has been reported to uptake 0.93 ton/m<sup>3</sup>, whereas MOF-210<sup>4</sup> exhibits a volumetric capacity of 0.72 ton/m<sup>3</sup> of CO<sub>2</sub> per volume of host material. Nevertheless, MOFs report the highest gravimetric capacity records because of their low density. Table 1 includes a comparison of exceptional results on CO<sub>2</sub> uptake - showing both volumetric and gravimetric values - and specifically our results on high volumetric capacity clays, calling the attention to the diversity of characteristics among all materials that could be combined for a viable carbon capture and storage solution.

Material	Mw	Cation	N**	N/cation ***	d <sub>001</sub> * not loaded	d <sub>001</sub> * loaded, 1st peak	d <sub>001</sub> * loaded, 2nd peak
Clay NiFh	791	Ni <sup>2+</sup>	5.1	8.5	10.9	12.1	13.1
Clay NaFh	773	Na <sup>+</sup>	3.6	3.0	9.6	12.3	—
Clay LiFh	754	Li <sup>+</sup>	2.8	2.3	10.3	11.9	—

**Table 2.** Fluorohectorite clay parameters. \*XRD data from previous work (Michels 2015) measured on samples of the same batch as in the present work; \*\*Number of CO<sub>2</sub> molecules captured per unit cell,  $N = (G/[Mw(CO_2)]/Mw(\text{clay}))$ ; \*\*\*Number of CO<sub>2</sub> molecules captured per cation,  $N/\text{cation} = (N/x)$ ;  $x = 0.6$  for Ni<sup>2+</sup>;  $x = 1.2$  for Li<sup>+</sup> and Na<sup>+</sup>.

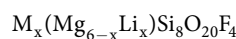
The other clay types investigated here, NaFh and LiFh, are also found to be high capacity storage materials, with intercalation capacity of 21 wt % (corresponding to 0.58 ton/m<sup>3</sup> or 4.7 mmol/g) and 16 wt % (corresponding to 0.46 ton/m<sup>3</sup> or 3.7 mmol/g), both at a final pressure of 53 bar respectively. These numbers are higher than those found in a theoretical study on other clays<sup>9</sup>, for example, Na-Montmorillonite with a capacity of 1.5 mmol/g for a basal interlayer distance of 12 Å, which is comparable with the interlayer distance of our loaded samples as shown in Table 2. The volumetric capacity of LiFh was already studied by us and published elsewhere<sup>23</sup>. Here we report new results on LiFh for a comparison using the same experimental protocol (dehydration, incubation time and incremental steps in pressure) as used for NiFh. The results for NiFh are original and demonstrate a significant development forward regarding CO<sub>2</sub> capture by a nano-silicate material.

NaFh and LiFh present very similar behavior in terms of the intercalation of CO<sub>2</sub>, as shown in Fig. 1. This suggests a similar interaction between the CO<sub>2</sub> molecule and the Na<sup>+</sup> and Li<sup>+</sup> cations. They are both alkali metals of group 1 A with comparable ionic distribution in the nano-silicate clay interlayers. Previous results showed that after the intercalation into Fluorohectorites, CO<sub>2</sub> is stable inside the nano-silicate clay material and can be released upon heating<sup>23</sup>, which indicates the formation of stable cation-CO<sub>2</sub> complexes or cation solvation into a CO<sub>2</sub> gas phase<sup>24</sup>. The size and structure of the complex might favor the stability and can be probed by X-ray diffraction (XRD). The XRD results from our previous work<sup>23</sup>, transcribed in Table 2, show that the interlayer separation occupied by CO<sub>2</sub> for NaFh and LiFh increases with the ionic radius of the cation. Na<sup>+</sup> has a larger ionic radius than Li<sup>+</sup>, and the loaded NaFh is found to have a larger interlayer separation than LiFh, which means additional room to accommodate a larger complex or higher coordination number. This could explain our finding that NaFh intercalates more CO<sub>2</sub> than LiFh at the investigated pressures.

The total CO<sub>2</sub> intercalated ( $\sum U_i$ ) as a function of pressure is shown in Fig. 1a, while Fig. 1b shows the incremental amount (U<sub>i</sub>) of CO<sub>2</sub> intercalated at each step in pressure. The latter indicates that the process is driven towards a saturation limit, after which no additional intercalation will be possible. Since the incremental values have not reached zero at the maximum pressure used in this study, it is possible that CO<sub>2</sub> intercalation is not yet at the full potential for this material. At this stage, despite presenting already a high uptake of CO<sub>2</sub>, further investigations into optimization of the CCS capacity of these materials may thus benefit from an extended pressure/temperature protocol as well as exploring the use of functionalized clays such as those prepared according to Breu's group<sup>25</sup>. Reuse of the CO<sub>2</sub>-loaded clay materials is possible after releasing the CO<sub>2</sub> by a combination of moderate heating and evacuation. This has been tested for NiFh, NaFh and LiFh (data not shown), with no sign of degradation of the material.

Table 1 shows the results for the CO<sub>2</sub> gravimetric and volumetric capacity for the clays studied in the present work, compared with Montmorillonite<sup>26</sup>, Zeolite 13X<sup>3</sup>, functionalized polymers<sup>5</sup>, activated carbons<sup>7</sup>, MOF-aminoclay composites<sup>11</sup> and MOF-210<sup>4</sup> data from the literature. The final pressure varies according to the characteristics of the material. Some materials, like the fluorohectorite clays, have low uptake for flue gas but are not saturated at low pressure, allowing storage at high pressure. Table 2 shows the molar weight, number of CO<sub>2</sub> molecules per unit cell (N) and the basal interlayer distance (d<sub>001</sub>) for each clay type.

The molecular formula per unit cell for NiFh, NaFh and LiFh is expressed by



where  $x = 1.2$  for LiFh ( $M = \text{Li}$ ) and NaFh ( $M = \text{Na}$ ) and  $x = 0.6$  for NiFh ( $M = \text{Ni}$ )<sup>27</sup>. The number N is found to be 5 in the case of NiFh. This means more than 8 molecules of CO<sub>2</sub> per Ni<sup>2+</sup> cation, since NiFh has approximately 0.6 Ni<sup>2+</sup> cations per unit cell<sup>28</sup>. The two other clays, LiFh and NaFh, contain 1.2 cation per unit cell, which gives a value for the ratio  $N/\text{cation}$  between 2 and 3.

The Fig. 2 shows possible structures of CO<sub>2</sub>-cation complexes assembled into NaFh and NiFh clay materials, respectively. These structures use as a starting point the crystal structure of water-containing clay, with cell parameters  $a = 5.2432$  Å and  $b = 9.0870$  Å, as published by Kalo *et al.*<sup>8</sup>, but here with the water molecules removed and substituted by another set of three atoms in the form of CO<sub>2</sub>. Our sketch of the CO<sub>2</sub> intercalated fluorohectorite is intended to give a plausible picture of how the CO<sub>2</sub> molecules could be arranged between the layers upon removal of water molecules. These hypothetical structures were derived by iterative process taking into account the nature of CO<sub>2</sub>-CO<sub>2</sub>, and CO<sub>2</sub>-host intercalations in a most qualitative way, while keeping interatomic distances from becoming too short. This was done without expanding the layer spacing from what it was for water. The three shortest CO<sub>2</sub> oxygen-to-host-oxygen distances were 2.31, 2.53 and 2.607 Å, but these can, of course, be readily increased by increasing the layer spacing. We have started with an interlayer distance of 10 Å, yielding a layer periodicity of 15 Å (as in Kalo *et al.*<sup>8</sup> for 2 water layers), which is close to the XRD results in the work of Michels *et al.*<sup>23</sup> and the simulations in the work of Kadoura *et al.* (2012)<sup>9</sup>. The configuration of the intercalated

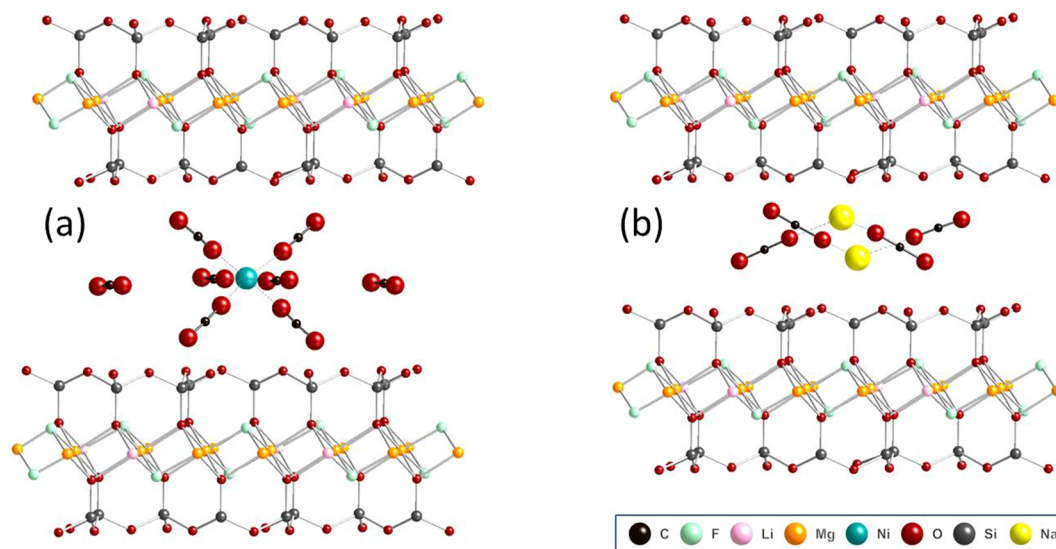


**Figure 2.** Suggested configuration for CO<sub>2</sub>-cation complexation inside Fluorohectorite clay interlayer: (a) 8 molecules of CO<sub>2</sub> for each Ni<sup>2+</sup> cation and (b) 2 molecules of CO<sub>2</sub> for each Na<sup>+</sup> cation. (The structures were built using the software CrystalMaker®).

complex is expected to be rather dynamic and the number of CO<sub>2</sub> molecules around each cation is here estimated to be 2 for NaFh and 8 for NiFh based on the amount of material intercalated. For free Ni<sup>2+</sup>, the coordination number<sup>29</sup> with CO<sub>2</sub> can be as high as 6, and in Fig. 2(a) we assume this to be the case for intercalated Ni<sup>2+</sup> as well. The binding of the two additional satellite molecules of CO<sub>2</sub> could come from interaction with the clay layers.

In conclusion, we have in this work compared alternative materials with exceptional gravimetric or volumetric capacity for CO<sub>2</sub> capture and storage. We have demonstrated that NiFh is able to capture 0.79 ton of CO<sub>2</sub> per m<sup>3</sup> of clay at 55 bar and ambient temperature. This is one of the highest volumetric capacities of all CO<sub>2</sub> sorbent material reported to date. This result, combined with the diversity of characteristics of other high performance materials, could lead to new technological solutions for Carbon Capture and Storage (CCS). The storage capacity for fluorohectorite clays may well be further enhanced beyond the present results by utilizing functionalized clay minerals<sup>8</sup>. Moreover, it has also been suggested that clay materials can be used in gas separation, in particular, those of greenhouse gases such as methane<sup>9</sup> from CO<sub>2</sub>.

Clay materials such as the synthetic Fluorohectorites investigated here are harmless<sup>30</sup> and in addition, their production is expected to be substantially less expensive than other high performance porous synthetic materials considered for CO<sub>2</sub> capture, such as MOFs whose upscaling is particularly challenging. Furthermore, clays are also proven to be highly stable when exposed to external mechanical stress or humidity on geological time scales.

Our results show that the type of clay-interlayer cation is critical for CO<sub>2</sub> capture, whereas the clay nanolayers provide the large effective surface area responsible for the exceptional storage capacity. The remarkable capture capacity of NiFh is also related to (a) a high charge density, about twice that of Montmorillonite<sup>28</sup>, and (b) the presence of divalent Ni<sup>2+</sup> that frees up additional space for CO<sub>2</sub> intercalation, which results in a higher uptake per cation compared with the usual monovalent ions such as Na<sup>+</sup>. The internal surface area for fluorohectorite and montmorillonite was found to be 3 m<sup>2</sup>/g and 80 m<sup>2</sup>/g respectively in the work of Kaviratna *et al.*<sup>28</sup> (using the fluorohectorite sample bought from the same batch as in the present work), which could be an indication that the CO<sub>2</sub> uptake, in these two clays, is more dependent on the interlayer separation and interlayer cation than on the internal surface area. We believe that the main interaction mechanism responsible for the high CO<sub>2</sub> affinity is direct dipolar electronic interaction with the interlayer cation. The physisorption is probably also, to some degree, influenced by the charge distribution of the clay layered structure.

Other aspects of sorption kinetics are under evaluation and DFT calculations of the intercalate CO<sub>2</sub>-cation structures are in progress using the initial model presented in Fig. 2 as starting point. This study will be combined with *in situ* spectroscopic characterization. Experiments using higher pressure, including liquid and supercritical CO<sub>2</sub>, are also planned. Our Sieverts apparatus allows for temperature measurements which will be important for future determination of heats of adsorption and comparisons with DFT calculations. The present work has been conducted on dehydrated clays; however it is of considerable interest to evaluate the sorption performance in the presence of water and selectivity for CO<sub>2</sub> in the presence of CH<sub>4</sub> and N<sub>2</sub>. The current results already make these materials highly interesting candidates for CO<sub>2</sub> capture from dried industrial combustion gases.

## Methods

We have utilized a custom-made Sieverts apparatus for the quantification of CO<sub>2</sub> storage capacity of the clay materials. The instrument has been designed and constructed for minimizing the experimental error and has been accurately calibrated according to procedures described in the literature<sup>31</sup>. CO<sub>2</sub> gas was introduced to the reservoir and equilibrated for one hour, prior to allowing the expansion into the sample chamber and intercalation into the clay powder material. The number of CO<sub>2</sub> gas molecules initially in the reservoir,  $n_i = P_i V_i / (Z_i R T_i)$ , gas molecules was calculated using the compressibility of a real gas,  $Z(p, T)$ , as a function of pressure and



temperature with parameters from NIST tables as reported elsewhere<sup>31</sup>. For each pressure increment, the gas uptake was calculated from the difference  $n_f - n_i$ , where  $n_f$  is the final number of gas molecules expanded to the total volume,  $V_f$  (sample chamber + reservoir):  $n_f = P_f(V_f - V_s)/(Z_fRT_f)$ , where  $V_s$ , sample volume, is the mass of sample per its bulk density. Prior to the gas sorption the clay powder was degassed for 20 hours at 120 °C under dynamic vacuum (down to 10<sup>-7</sup> mbar), and the subsequent experiments were performed at 25 °C. The synthetic clays Nickel Fluorohectorite (NiFh), Sodium Fluorohectorite (NaFh) and Lithium Fluorohectorite (LiFh) and CO<sub>2</sub> gas with purity >99.999% was used. LiFh was purchased from Corning Inc. NiFh and NaFh powder samples were obtained from the LiFh clay following a standard dialysis cation exchange protocol<sup>32</sup> with no further analysis. Water intercalation in NaFh and NiFh samples, originated from the same LiFh batch that we have studied here, have been investigated by NMR spectroscopy (NaFh<sup>29</sup>), and TGA (NiFh<sup>19</sup>). The cation coordination numbers proposed from these results are in full accordance with the clay layer charge reported by Kaviratna *et al.*<sup>28</sup>.

The Sieverts apparatus had a reservoir volume of 16 ml and sample chamber of 13 ml. We have determined the number of CO<sub>2</sub> molecules at the reservoir before and after expansion of the reservoir into the sample chamber. The whole process consisted of three stages: (A) degassing of sample and chambers, (B) accumulation of CO<sub>2</sub> into the reservoir at a certain incremental step in pressure and, finally, (C) expansion of CO<sub>2</sub> into the sample chamber. The total CO<sub>2</sub> intercalation was determined as a sum of the intercalation amounts due to each incremental step in pressure. The CO<sub>2</sub> intercalation was replicated for testing reproducibility. The amount of powder sample inside the chamber was around 2 g and the bulk density around 0.7 g/ml. The total intercalation period, steps 1 to 3, was uniform around 4 days for all samples. Previous experiments<sup>22</sup> showed that the kinetics of intercalation is slower for NaFh compared to NiFh and LiFh, so we chose to expose all samples to the longest period. We expect that the intercalation time might reduce under different conditions, for example with supercritical CO<sub>2</sub>.

## References

- Nugent, P. *et al.* Porous materials with optimal adsorption thermodynamics and kinetics for CO<sub>2</sub> separation. *Nature* **495**, 80–84 (2013).
- Vitillo, J. G., Smit, B. & Gagliardi, L. Introduction: Carbon Capture and Separation. *Chem. Rev.* **117**, 9521–9523 (2017).
- Cavenati, S., Grande, C. A. & Rodrigues, A. E. Adsorption Equilibrium of Methane, Carbon Dioxide, and Nitrogen on Zeolite 13X at High Pressures. *J. Chem. Eng. Data* **49**, 1095–1101 (2004).
- Furukawa, H. *et al.* Ultrahigh Porosity in Meta-Organic Frameworks. *Science* (80-.). **329**, 424 (2010).
- Rukmani, S. J., Liyana-arachchi, T. P., Hart, K. E. & Colina, C. M. Ionic-Functionalized Polymers of Intrinsic Microporosity for Gas Separation Applications. *Langmuir*, <https://doi.org/10.1021/acs.langmuir.7b04320> (2018).
- Hart, K. E. & Colina, C. M. Ionomers of Intrinsic Microporosity: In Silico Development of Ionic- Functionalized Gas-Separation Membranes (2014).
- Cox, M. & Mokaya, R. Sustainable Energy & Fuels Ultra-high surface area mesoporous carbons for colossal pre combustion CO<sub>2</sub> capture and storage as materials for hydrogen purification. *Sustain. Energy Fuels* **1**, 1414–1424 (2017).
- Kalo, H., Milius, W. & Breu, J. Single Crystal Structure Refinement of One- and Two-layer Hydrate of Sodium-Fluorohectorite. *Supplementary* 1–5 (2012).
- Kadoura, A., Narayanan Nair, A. K. & Sun, S. Adsorption of carbon dioxide, methane, and their mixture by montmorillonite in the presence of water. *Microporous Mesoporous Mater.* **225**, 331–341 (2016).
- Romanov, V. N. Evidence of irreversible CO<sub>2</sub> intercalation in montmorillonite. *Int. J. Greenh. Gas Control* **14**, 220–226 (2013).
- Chakraborty, A., Achari, A., Eswaramoorthy, M. & Maji, T. K. MOF-aminoclay composites for superior CO<sub>2</sub> capture, separation and enhanced catalytic activity in chemical fixation of CO<sub>2</sub>. *Chem. Commun.* **52**, 11378–11381 (2016).
- Mukherjee, S. *The Science of Clays. The Science of Clays: Applications in Industry, Engineering and Environment*, <https://doi.org/10.1007/978-94-007-6683-9> (Springer Netherlands, 2013).
- Hansen, E. L. *et al.* Swelling transition of a clay induced by heating. *Sci. Rep.* **2**, 1–2 (2012).
- Kalo, H., Möller, M. W., Ziadeh, M., Dolejš, D. & Breu, J. Large scale melt synthesis in an open crucible of Na-fluorohectorite with superb charge homogeneity and particle size. *Appl. Clay Sci.* **48**, 39–45 (2010).
- Breu, J., Seidl, W., Stoll, A. J., Lange, K. G. & Probst, T. U. Charge homogeneity in synthetic fluorohectorite. *Chem. Mater.* **13**, 4213–4220 (2001).
- da Silva, G. J., Fossum, J. O., DiMasi, E. & Måløy, K. J. Hydration transitions in a nanolayered synthetic silicate: A synchrotron x-ray scattering study. *Phys. Rev. B* **67**, 094114 (2003).
- Jiménez-Ruiz, M., Ferrage, E., Delville, A. & Michot, L. J. Anisotropy on the Collective Dynamics of Water Confined in Swelling Clay Minerals. *J. Phys. Chem. A* **116**, 2379–2387 (2012).
- Martins, M. L. *et al.* Neutron scattering, a powerful tool to study clay minerals. *Appl. Clay Sci.* **96**, 22–35 (2014).
- Altoé, M. A. S. *et al.* Continuous water adsorption states promoted by Ni<sup>2+</sup> confined in a synthetic smectite. *Appl. Clay Sci.* **123**, 83–91 (2016).
- Loring, J. S. *et al.* Clay Hydration/dehydration in Dry to Water-saturated Supercritical CO<sub>2</sub>: Implications for Caprock Integrity. *Energy Procedia* **37**, 5443–5448 (2013).
- Giesting, P., Guggenheim, S., Koster van Groos, A. F. & Busch, A. X-ray Diffraction Study of K- and Ca-Exchanged Montmorillonites in CO<sub>2</sub> Atmospheres. *Environ. Sci. Technol.* **46**, 5623–5630 (2012).
- Hemmen, H. *et al.* X-ray studies of carbon dioxide intercalation in Na- fluorohectorite clay at near-ambient conditions. *Langmuir* **1–4** (2012).
- Michels, L. *et al.* Intercalation and retention of carbon dioxide in a smectite clay promoted by interlayer cations. *Sci. Rep.* **5**, 8775 (2015).
- Criscenti, L. J. & Cygan, R. T. Molecular simulations of carbon dioxide and water: Cation solvation. *Environ. Sci. Technol.* **47**, 87–94 (2013).
- Stöter, M. *et al.* Nanoplatelets of sodium hectorite showing aspect ratios of ≈20 000 and superior purity. *Langmuir* **29**, 1280–1285 (2013).
- Stevens, L. *et al.* Preparation and CO<sub>2</sub> adsorption of diamine modified montmorillonite via exfoliation grafting route. *Chem. Eng. J.* **215–216**, 699–708 (2013).
- Besson, G., Mifsud, A., Tchoubar, C. & Mering, J. Order and disorder relations in the distribution of the substitutions in smectites, illites and vermiculites. *Clays Clay Miner.* **22**, 379–384 (1974).
- Kaviratna, P. D., Pinnavaia, T. J. & Schroeder, P. A. Dielectric properties of smectite clays. *J. Phys. Chem. Solids* **57**, 1897–1906 (1996).
- Tejedor-Tejedor, M. I., Anderson, M. A. & Herbillon, A. J. An investigation of the coordination number of Ni<sup>2+</sup> in nickel bearing phyllosilicates using diffuse reflectance spectroscopy. *J. Solid State Chem.* **50**, 153–162 (1983).

30. dos Santos, E. C. *et al.* Ciprofloxacin intercalated in fluorohectorite clay: identical pure drug activity and toxicity with higher adsorption and controlled release rate. *RSC Adv.* **7**, 26537–26545 (2017).
31. Policicchio, A. *et al.* Volumetric apparatus for hydrogen adsorption and diffusion measurements: Sources of systematic error and impact of their experimental resolutions. *Rev. Sci. Instrum.* **84** (2013).
32. Knudsen, K. D., Fossum, J. O., Helgesen, G. & Bergaplass, V. Pore characteristics and water absorption in a synthetic smectite clay. *J. Appl. Crystallogr.* **36**, 587–591 (2003).

### Acknowledgements

This work was supported by the Norwegian Research Council under the Frinatek Program, project number 250728, using the laboratories of Jeep II Neutron facility at Kjeller, and the Laboratory for Soft and Complex Matter Studies at the Department of Physics, NTNU in Trondheim, Norway.

### Author Contributions

J.O.F. initiated and planned the work together with K.D.K. G.N.K. aided L.P.C. in the initial phase of the experiments and analysis. J.E. constructed the numerical CO<sub>2</sub>-cation complexation representations. L.P.C. performed the experiments, analysis and wrote the first draft of the manuscript. All authors took active part in revisions and discussions towards the final manuscript.

### Additional Information

**Competing Interests:** The authors declare no competing interests.

**Publisher's note:** Springer Nature remains neutral with regard to jurisdictional claims in published maps and institutional affiliations.



**Open Access** This article is licensed under a Creative Commons Attribution 4.0 International License, which permits use, sharing, adaptation, distribution and reproduction in any medium or format, as long as you give appropriate credit to the original author(s) and the source, provide a link to the Creative Commons license, and indicate if changes were made. The images or other third party material in this article are included in the article's Creative Commons license, unless indicated otherwise in a credit line to the material. If material is not included in the article's Creative Commons license and your intended use is not permitted by statutory regulation or exceeds the permitted use, you will need to obtain permission directly from the copyright holder. To view a copy of this license, visit <http://creativecommons.org/licenses/by/4.0/>.

© The Author(s) 2018